doi: 10.1115/ICEF2019-7159 Pre-Print

Proceedings of the ASME 2019 Internal Combustion Engine Fall Technical Conference
ICEF2019
October 20-23, 2019, Chicago, IL, USA

IMPLEMENTING NATURAL GAS IN A COMPRESSION IGNITION CYCLE USING NOBLE GAS ADDITION

Martia Shahsavan
Dept. of Mechanical Engineering
University of Massachusetts Lowell
Lowell, MA, USA

Mohammadrasool Morovatiyan
Dept. of Mechanical Engineering
University of Massachusetts Lowell
Lowell, MA, USA

Mammadbaghir Baghirzade
Dept. of Mechanical Engineering
University of Massachusetts Lowell
Lowell, MA, USA

J. Hunter Mack
Dept. of Mechanical Engineering
University of Massachusetts Lowell
Lowell, MA, USA

ABSTRACT

Natural gas is known as a relatively clean fossil fuel due to its low carbon to hydrogen ratio compared to other transportation fuels, which yields a reduction of carbon monoxide, carbon dioxide, and unburned hydrocarbons emissions. However, it has a low cetane number, which makes it a difficult fuel for use in compression ignition engines. A potential solution for this issue can be adding small amounts of argon, as a noble gas with a low specific heat to modify the intake conditions. In this numerical study, a commercial compression ignition engine has been modeled to evaluate the auto-ignition of natural gas with the modified intake conditions. Different amounts of argon added to the intake air are examined in order to attain the optimal operating conditions. A detailed chemistry solver is implemented on a 53-species chemical kinetics mechanism to calculate the rate constants. The results show that compression ignition of natural gas can be achieved by adding small amounts of argon to the intake air. It drastically increases the in-cylinder temperature and pressure near TDC, which enables the auto-ignition of the injected natural gas. Moreover, it leads to the reduction in ignition delay and heat release rate, and expands the combustion duration. Emissions analysis indicates that NOx and CO_2 can be significantly diminished by increasing the amount of argon in the intake composition. This study introduces an efficient and clean compression ignition engine fueled with natural gas running in optimal operating conditions using argon addition to the intake.

Keywords: Natural Gas, Noble Gases, Clean Combustion, Argon Power Cycle, Compression Ignition Engine

1. INTRODUCTION

The use of natural gas in internal combustion engines produces less CO_2, CO, and HC emissions compared to the other common fossil fuels due to the relatively low carbon to hydrogen ratio [1]. Moreover, it possesses a high octane number (~120 - 130), which enables the engine to run at a higher compression ratio and achieve a higher thermodynamic efficiency [2]. Natural gas has relatively wide flammability limits, which allows for operation at ultra-lean conditions [3, 4]. The significantly large proven reserves of natural gas (200 trillion cubic meters worldwide) combined with the capability to operate a cleaner and more efficient cycle make it an attractive alternative fuel [5]. The use of natural gas as a standalone fuel, or as a blend with diesel or hydrogen, has been extensively studied in traditional spark ignition engines [6-9] and more advanced cycles such as homogeneous charge compression ignition (HCCI) [10-14] and reactivity controlled compression ignition (RCCI) [15-18].

Compression ignition cycles generally have a higher thermodynamic efficiency due to the ability to operate at a higher compression ratio. However, investigations on natural gas compression ignition engines are quite limited due to its low cetane number [19]. It is practically impossible to auto-ignite natural gas in common compression ignition engines since high in-cylinder temperatures are required. A number of studies tried to introduce a solution by using a secondary fuel such as diesel [20-22], hydrogen [23], rapeseed methyl ester (RME) [24], dimethyl ether (DME) [25], and methyl propanoate (MP) [26]. An alternative approach is using noble gases as the working fluid

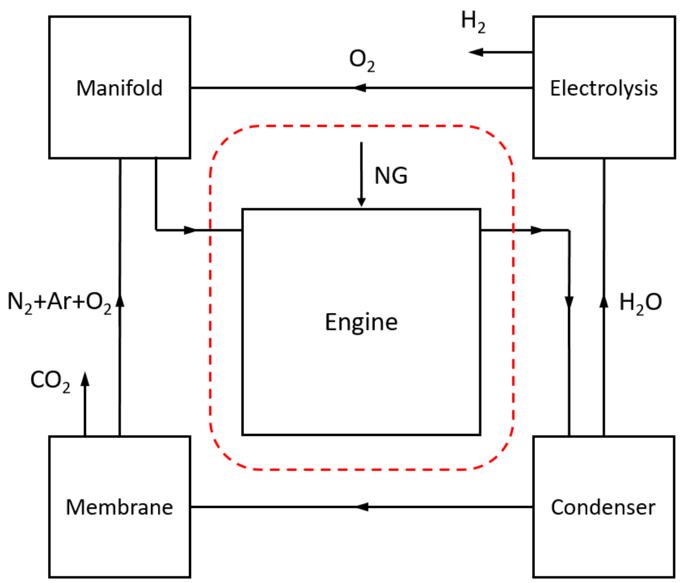

Figure 1. Argon assisted natural gas compression ignition engine. The scope of this study is specified by the dashed box.

to increase the in-cylinder temperature. Among the noble gases, argon has proven to be the leading choice due to the accessibility and a relatively lower cost. Argon possesses a lower specific heat compared to nitrogen. Thus, it theoretically yields higher temperatures at TDC in comparison to nitrogen, the primary component of air. Additionally, argon has a higher specific heat ratio (1.67) compared to nitrogen (1.40), which increases the ideal thermodynamic efficiency. A number of studies have assessed the use of argon in engines as the working fluid [27, 28]. Argon is shown to be capable of decreasing the ignition delay and increasing the in-cylinder temperature [29, 30]. Moreover, the theoretical thermal efficiency can be increased up to 20% when compared to the conventional engines using nitrogen as the working fluid [31].

The current study aims to evaluate the feasibility of using natural gas as a standalone fuel in a compression ignition engine with partial replacement of nitrogen by argon. Figure 1 shows a schematic diagram of the hypothetical argon assisted natural gas compression ignition engine. Nitrogen, argon, and oxygen are introduced to the engine through the inlet manifold, and natural gas is directly injected into the comparably high temperature air, and auto-ignites. Due to the extremely lean operating condition and the excess amount of oxygen, the products mainly include nitrogen, argon, oxygen, and slight amounts of water vapor and carbon dioxide. The water vapor can be readily condensed, and separated to hydrogen and oxygen through an electrolysis procedure. The oxygen can be recirculated to the inlet manifold to compensate the amount of consumed oxygen in the cylinder during the combustion process. The carbon dioxide in the products can be separated using a proper membrane, and the remaining gases including nitrogen, argon, and oxygen return to the inlet manifold for the next cycle. The feasibility, cost, energy efficiency, and system analysis of this hypothetical cycle should

Table 1. Engine Specifications

Parameters	Specifications
Engine type	YANMAR NF19SK
Type of cylinder head	Disc
Bore × Stroke (mm)	110 × 106
Engine speed (rpm)	1200
Compression ratio	14:1
Fuel	Natural gas
Oxygen concentration (by vol.)	21%
Argon addition to nitrogen (by vol.)	0 - 80%
Overall equivalence ratio	0.09
Initial pressure (bar)	1.14
Initial temperature (K)	400
Injector pressure (bar)	80
Start of injection (°CA)	-15 aTDC
Injection duration (°CA)	10
Nozzle diameter (mm)	0.8

Table 2. Composition of natural gas

Component	Mole fraction (%)
Methane (CH_4)	94.0
Ethane (C_2H_6)	4.2
Nitrogen (N_2)	1.0
Carbon Dioxide (CO_2)	0.5
Propane (C_3H_8)	0.3

be investigated. However, the scope of this study as shown in Figure 1 is confined to the combustion process inside the engine. For this objective, numerical simulation is chosen as a rational first step to explore the numerous input and output parameters associated with the non-premixed combustion of natural gas in the specified engine.

2. MATERIALS AND METHODS

A numerical simulation is carried out in order to examine the capability of natural gas as a fuel in compression ignition cycles, and to understand its combustion characteristics in argon-nitrogen-oxygen mixtures. The YANMAR NF19SK engine is selected with the parameters given in Table 1. Previously, experimental studies on non-premixed combustion of hydrogen in argon-oxygen mixtures were conducted in this engine [32], and the experimental data are available to validate the current numerical modeling [33]. Most of the operating conditions such as initial temperature, initial pressure, and injection pressure are kept the same. However, the engine speed is changed from 600 rpm to 1200 rpm, which is within the normal speed range of natural gas engines. The injection duration is increased from 5 °CA to 10 °CA for optimization of the combustion process.

The overall equivalence ratio is calculated as 0.09, which means the engine runs at an extremely lean operating condition. This provides an excess amount of oxygen in products, which can be

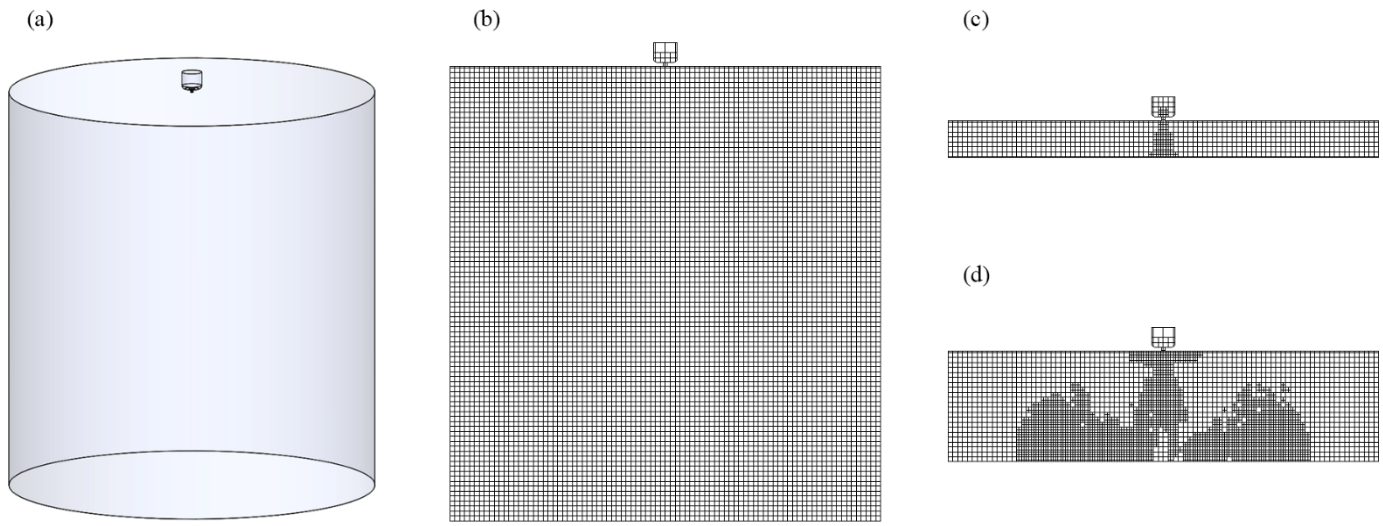

Figure 2. (a) Geometry of the model, **(b)** Grid configuration on a slice of the model, **(c)** Fixed embedding on the nozzle and near nozzle areas during injection, **(d)** Adaptive mesh refinement during combustion and flame propagation.

recirculated to the inlet manifold through EGR. Natural gas is introduced in the modeling using five of its main components, methane, ethane, nitrogen, carbon dioxide, and propane with the mole fractions indicated in Table 2. Different amounts of argon replacement from 10% to 80% by volume are investigated, and the results are compared against no argon replacement, when nitrogen is the only working fluid. All concentrations including argon replacement written in this paper are based on volume.

2.1. Numerical Simulation

This study is conducted in CONVERGE CFD software, a powerful tool designed specifically for internal combustion engine applications. It automatically generates orthogonal grids, which is a huge advantage in complex and detailed geometries such as engines. The geometry of the current study is created in a 3D CAD software, and imported into CONVERGE. Figure 2 shows the geometry and the grid configuration of the model. The simulation is based on a closed cycle, meaning the duration between intake valve close (IVC) and exhaust valve open (EVO). The domain consists of two different regions: (1) injector, which involves natural gas at 80 bar and 400 K, and (2) cylinder containing oxygen-nitrogen-argon mixture at initial pressure and temperature of 1.14 bar and 400 K. The simulation begins when the piston is at BDC, and the two regions are disconnected until -15 °CA aTDC when the injection starts, and the natural gas enters the cylinder due to the pressure gradient. At -5 °CA aTDC, the injection ends by detaching the two regions. To increase the computational efficiency, a relatively coarse base grid (5 mm) is selected, and mesh refinement is implemented using a fixed embedding on the nozzle and near nozzle areas, and adaptive mesh refinement (AMR) on velocity and temperature. AMR automatically splits a cell if gradients exceed a certain user-defined value (1 m/s and 2.5 K here). Figure (d) shows how the grid configuration changes during the injection and combustion where large gradients of velocity and temperature appear in the solution. A sensitivity analysis for the grid resolution is carried out, and the results are presented in Table 3. A base grid size of 5 mm with a permanent embedding scale of 2 (1.25 mm), and a sequential embedding scale of 2 (1.25 mm) for injector, and 3 (0.625 mm) for near nozzle areas during the injection event provide an optimized and reliable grid configuration. Higher levels of embedding result in the same mass of injected gas, and increase the computational cost.

Table 3. Grid embedding sensitivity analysis. A base grid size of 5 mm and embedding levels of 2 and 3 (underlined) for the injector and near nozzle areas are chosen to create the optimized grid configuration.

Embedding Level Injector/Near nozzle	Injected Mass (kg)	Overall Equivalence Ratio
0 / 1	6.00×10^{-6}	0.07
1 / 2	6.92×10^{-6}	0.08
<u>2 / 3</u>	$\underline{7.08\times10^{-6}}$	<u>0.09</u>
3 / 4	7.08×10^{-6}	0.09
4 / 5	7.09×10^{-6}	0.09

For gas simulation, a Redlich-Kwong equation of state is used since it provides a more realistic result compared to the ideal gas law. The SAGE detailed chemistry solver is employed, which simulates the combustion by calculation of reaction rates of each elementary reaction using well-known Arrhenius equation:

$$k = AT^b e^{(-E_a/R_u T)} \tag{1}$$

where A (pre-exponential factor), b (temperature exponent), and E_a (activation energy) are empirical parameters. For chemical kinetics, a CHEMKIN format GRI-Mech 3.0 mechanism

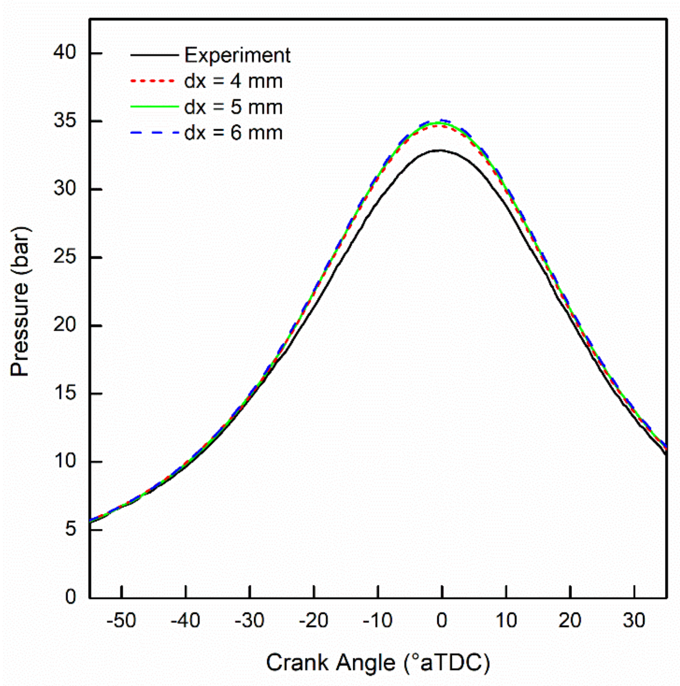

Figure 3. Comparison of the modeling and experimental results. dx shows the base grid size.

including 53 species and 325 reactions is introduced to the modeling. A varied time step with a minimum of 1×10^{-8} s, a maximum of 1×10^{-4} s, and a maximum convective CFL (Courant-Friedrichs-Lewy) limit of 1.0 is used to regulate the time step when required. For turbulence, a RNG k-ε (Re-normalization group) RANS (Reynolds-averaged Navier-Stokes) model is used to calculate the turbulent kinetic energy and dissipation rate at a relatively moderate computational cost.

2.2. Model Validation

In order to validate the numerical results, an experiment on the same engine involving 21% oxygen and 79% argon, and operating at 600 rpm with a compression ratio of 10 is simulated. The pressure trace is then compared against the experimental data [32]. Three different base grid sizes of 4, 5, and 6 mm are evaluated, and the results are shown in Figure 3. The error in prediction of the peak pressure is 4.4%, 4.6%, and 5.1% respectively. Based on this result, the base grid size of 5 mm is selected for the entire study since it possesses a good level of agreement with the experimental data.

3. RESULTS AND DISCUSSION

Nine different intake gas compositions ranging from 0% argon replacement (air) to 80% argon replacement are assumed for comparison of the combustion characteristics of natural gas. The oxygen concentration is kept constant (21%) in all cases. The effect of argon addition on pressure, temperature, heat release rate (HRR), ignition delay, and emissions is investigated, and the results are extensively discussed.

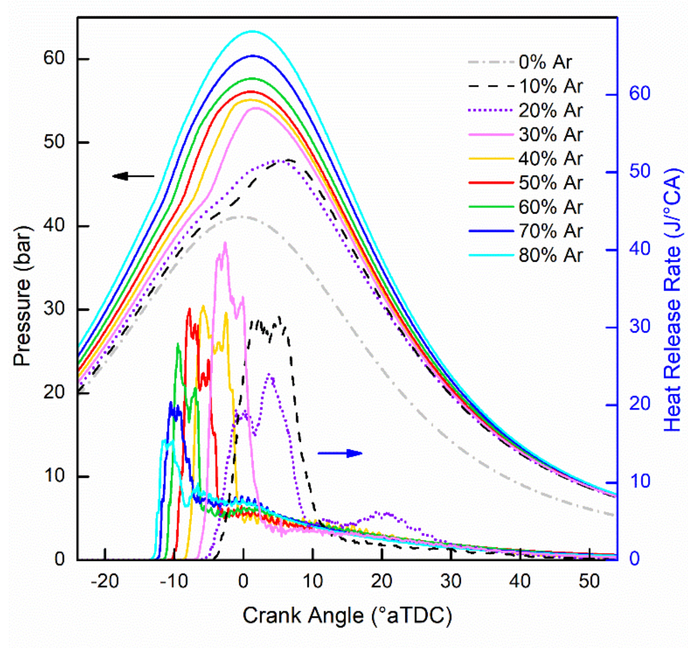

Figure 4. Pressure and HRR at different argon addition conditions.

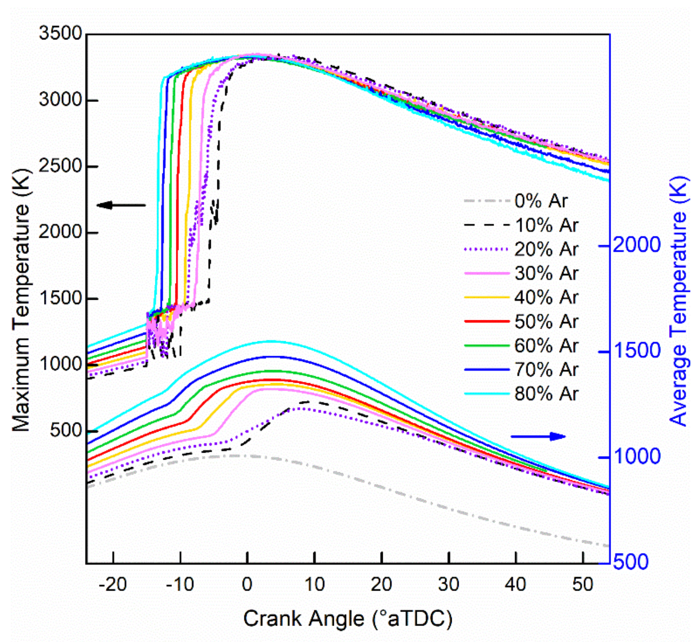

Figure 5. Maximum and average temperature at different argon addition conditions.

3.1. Combustion Characteristics

The resulted pressure and heat release rate curves are shown in Figure 4. The case in which nitrogen (0% argon addition) was the working fluid does not ignite, as expected. However, all other cases yield ignition of the natural gas and combustion inside the engine. However, the cases with at least 30 percent argon addition indicate more practical curves compared to 10 and 20 percent. Increasing the amount of argon in the intake

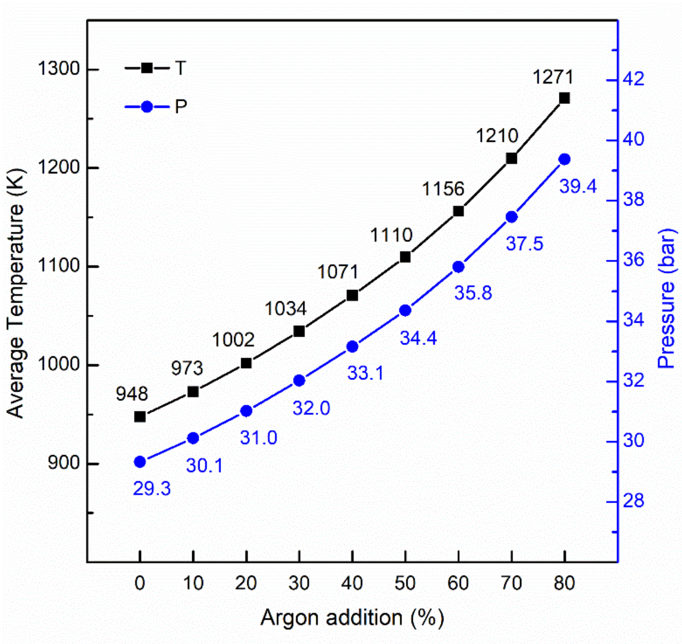

Figure 6. In-cylinder pressure and average temperature at start of injection (-15 °CA aTDC) at different argon addition conditions.

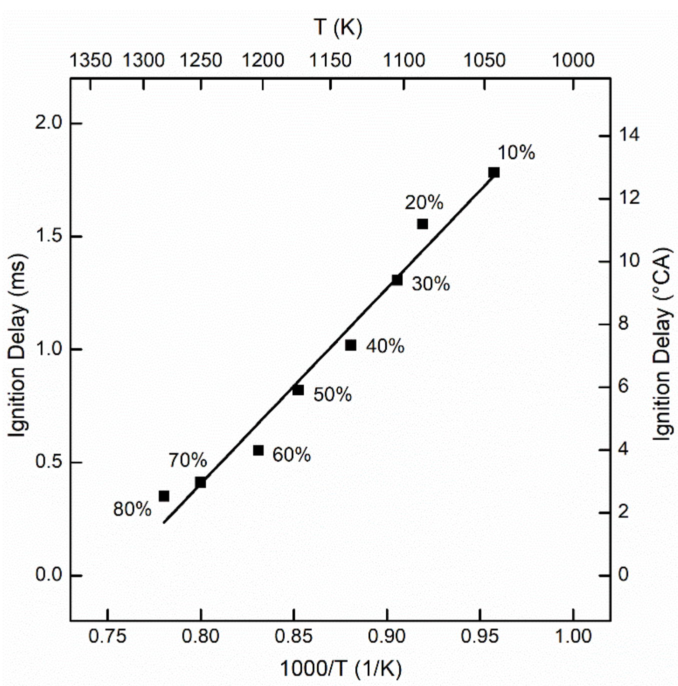

Figure 7. Ignition delay versus average temperature. The percentages on data points represent nitrogen replacement by argon.

composition leads to an earlier combustion and a higher peak pressure. Additionally, it extends the combustion duration. The heat release rates however show a more complex behavior with respect to the argon addition. The lowest peak heat release rate belongs to the 80 percent argon addition (~16 J/°CA), and the highest peak heat release rate occurs when 30 percent of nitrogen is replaced by argon (~41 J/°CA). Increasing the amount of argon above 30 percent reduces the peak heat release rate, and accelerates the onset of combustion. For 10 and 20 percent argon addition, the pressure and heat release rates show abnormal combustion with a low and extremely late heat release. The average and maximum temperature in the domain are shown in Figure 5, which are completely in agreement with the pressure and heat release rate data. As seen, the average temperature increases with addition of argon in the inlet gas composition. The maximum temperature as an appropriate representative of ignition indicates that decreasing the amount of argon delays the onset of combustion due to the lower in-cylinder temperature before TDC when the natural gas is injected. The first jump in the maximum temperature curve is due to the opening of the nozzle and start of injection at -15 CA aTDC. When the nozzle opens, a high pressure stream of natural gas enters into the cylinder and creates a high speed flow. Therefore, the temperature of some near nozzle areas slightly increases due to the high speed flow of the injected gas and the mixing process. Fluid mechanics and gas dynamics cause this jump in the maximum temperature curve. Thus, it does not affect the HRR curve. Due to the extremely lean operating condition (0.09), the average temperature is not severely high. This aids to the reduction of NOx, which is discussed in the emissions section of this paper.

In order to have an explicit understanding of the effect of argon addition on the auto-ignition of natural gas, the in-cylinder pressure and temperature at start of injection (SOI) are recorded and plotted as shown in Figure 6. At -15 °CA aTDC when the injection begins, the pressure is 29.3 bar if only nitrogen and oxygen exist in the cylinder. Replacing 50 percent of nitrogen by argon increases the pressure at SOI to 34.4 bar (~17%). This pressure can further advance to 39.4 bar (~34%) if 80 percent of nitrogen replaces by argon. More importantly, the average in-cylinder temperature at SOI, which is a decisive parameter in auto-ignition, boosts from 948 K in case of no argon to 1110 K with 50 percent and 1271 K with 80 percent argon addition. This is due to the lower specific heat of argon compared to nitrogen, which enables the mixture to attain a higher temperature and facilitates the auto-ignition of natural gas. Both temperature and pressure graphs are concave upward, which implies that the effect of argon addition on in-cylinder temperature and pressure is increasing. Figure 7 shows the ignition delay versus average temperature for varied argon addition cases. Ignition delay can be calculated using the extrapolation of the maximum slope of the pressure, temperature, or heat release rate back to the start of injection condition. In this study, heat release rate was used for calculation of the ignition delay. For 10 and 20 percent argon addition when the temperature is less than 1100 K, a quite long ignition delay is observed (more than 1.5 ms or 10 °CA). Increasing the amount of argon in the intake composition reduces the ignition delay. For 40 percent argon addition, the ignition delay is slightly more than 1 ms (7 °CA), and for 60 percent and above argon addition, the ignition delay becomes significantly

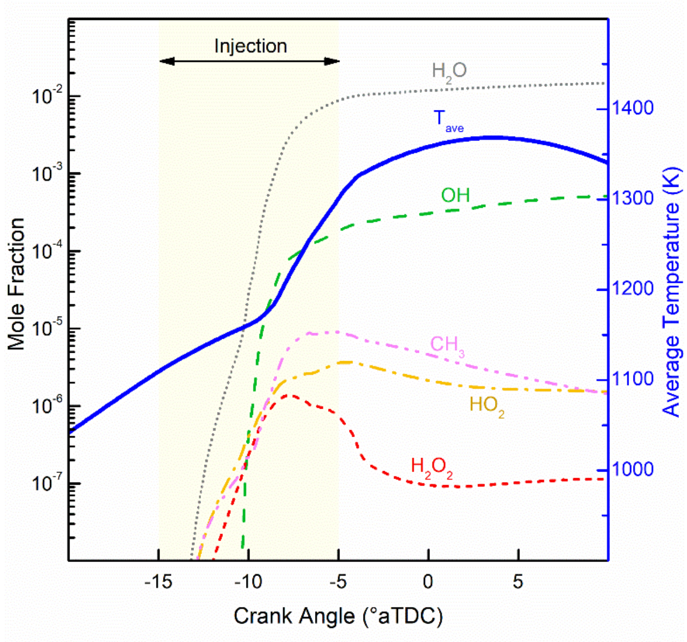

Figure 8. History of species mole fractions during combustion stage at 50% argon addition condition.

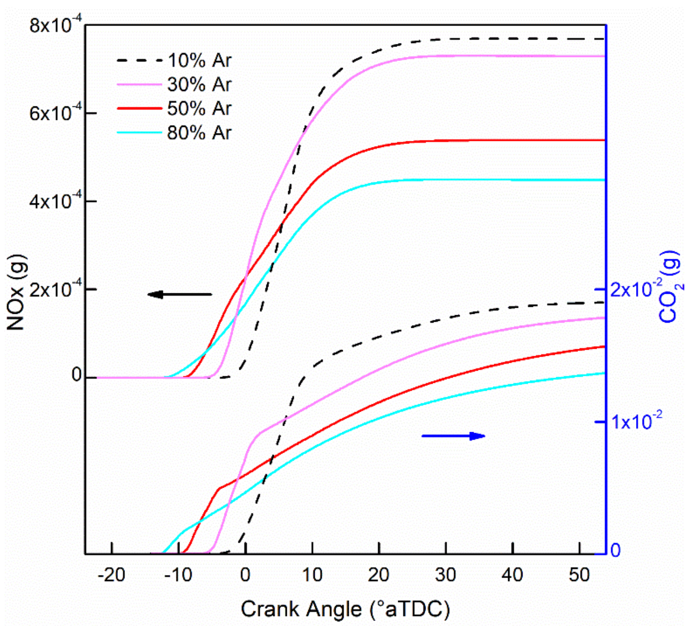

Figure 9. Comparison of emissions at different argon addition conditions.

shorter (less than 4 °CA). This is due to the relatively higher temperature (above 1200 K) for these cases. As seen, the desired ignition delay can be readily regulated by changing the concentration of argon in the intake gas composition.

3.2. Species and emissions

Numerical simulations can enable the investigation on the history of species during ignition and combustion development

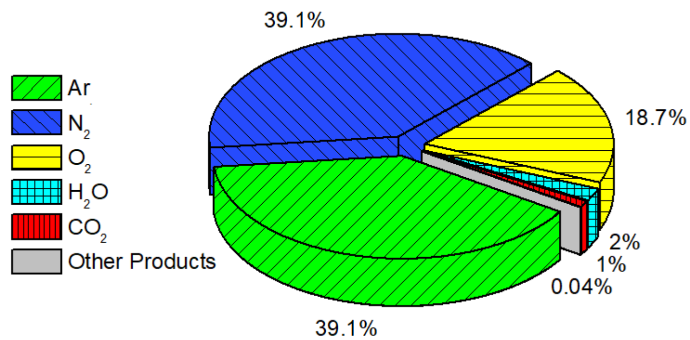

Figure 10. Mole fractions of the products at 50% argon addition condition.

without requiring intricate and costly optical measurement methods. Implementation of a reliable chemical kinetics mechanism such as GRI-Mech 3.0 on the CFD modeling combined with the adaptive mesh refinement and an established chemistry solver such as SAGE are sufficient for acquiring informative data on species production and consumption. Figure 8 shows the history of crucial species and radicals along with the recorded average temperature for the 50 percent argon addition case. The injection duration is highlighted for a better understanding of the species development. The average temperature at SOI (-15 °CA aTDC) is slightly above 1100 K, and it reaches a maximum of 1368 K. For intermediate temperature ignition applications such as compression ignition, homogeneous charge compression ignition (HCCI), rapid compression machines (RCM), and engine knock studies, key reactions are as following [34]:

$$H + O_2 + M \rightarrow HO_2 + M \tag{2}$$

$$CH_4 + HO_2 \rightarrow CH_3 + H_2O_2 \tag{3}$$

$$H_2O_2 + M \rightarrow OH + OH + M \tag{4}$$

$$CH_4 + OH \rightarrow CH_3 + H_2O \tag{5}$$

where M is a third body, CH_4 is a representative for alkanes, and CH_3 is an example of an alkyl radical. After start of injection, HO_2 and H_2O_2 radicals are produced through reactions 2 and 3. These two radicals are associated with the low temperature heat release. They maintain growing with the temperature increase due to the compression in the cylinder. At about 1150 K when the crank angle is roughly -8 aTDC, H_2O_2 breaks rapidly, and generates OH radicals (reaction 4). This is believed to be the key reaction for ignition since two OH radicals are produced in a quite short time. Figure 8 indicates that the change of slope in the temperature curve is completely synced with the H_2O_2 decomposition, which is in agreement with the literature [35]. With production of OH, the fuel which is mainly methane reacts with OH and generates an alkyl (CH_3) and water vapor (reaction 5). The results indicate that reactions 4 and 5 are decisive for prediction of ignition and onset of combustion.

Since this engine is operated at an extremely lean condition, near zero unburned hydrocarbons are observed in the products, and the only emissions produced are CO_2 and NOx, which are plotted versus crank angle in Figure 9. In order to prevent confusion caused by redundant crossing curves, only four cases involving 10, 30, 50, and 80 percent argon addition are presented to understand the generic effect of nitrogen replacement by argon on the production of emissions. Both CO_2 and NOx emerge earliest at 80 percent condition followed by 50, 30, and 10 percent, which is in agreement with the start of combustion for these cases. After ignition, CO_2 and NOx concentrations in the cylinder increase immediately. The most rapid growth of CO_2 and NOx is observed at 30 percent argon addition, which possesses the highest peak of heat release as seen in Figure 4. The production of NOx and CO_2 continues at a slower speed with the drop of heat release rate, and ends when the heat release rate becomes zero. The final mass of the emissions has a reverse correlation with the amount of argon added in the inlet composition. This means that the 10 percent case produces the largest amounts of emissions followed by 30, 50, and 80 percent argon addition cases. The result indicates that the replacement of nitrogen by argon does not exclusively reduce the NOx emissions due to the decrease in the number of nitrogen atoms, it additionally diminishes the CO_2 emission in products.

The final products of the 50 percent argon addition case are illustrated as a pie chart in Figure 10. The major products include argon (39.1%), nitrogen (39.1%), and oxygen (18.7%). This indicates that the hypothesis of recirculating the excess oxygen to the inlet manifold due to the extremely lean condition is practical. Water vapor and carbon dioxide are the following products with 2 and 1 percent mole fraction, and the other products including NOx are quite negligible (0.04%). The composition of the products implies the feasibility of a relatively clean compression ignition engine using natural gas as the fuel and argon as the addition to the working fluid.

Although the results of this study indicate a clean and efficient compression ignition of natural gas, more investigations are required to optimize the combustion characteristics and emission analysis. The calculated indicated mean effective pressure (IMEP) for different argon addition cases vary between 1.7 to 2.2 bar, which is relatively low. However, this modeling is at quite lean operating condition (about 0.1 equivalence ratio), and such an IMEP range is expected. An enhanced IMEP can be achieved by increasing the overall equivalence ratio using a multi-hole injector. On the other hand, increasing the injection pressure can cause a greater mass of fuel, which leads to a richer operating condition and consequently a higher IMEP. There are numerous parameters which can significantly affect the combustion process including running the engine at different compression ratios, varied intake temperatures, and boosted intake conditions. Furthermore, a specific injector design for natural gas can expand the range of the overall equivalence ratio. The lower density of natural gas compared to common liquid fuels used in compression ignition engines such as diesel yields smaller amount of the injected fuel. Optimization of the injector such as the number of nozzles, size of nozzles, and injection pressure can overcome this issue. Finally, a comprehensive system analysis is essential to assess the performance and efficiency of the hypothetical argon assisted natural gas compression ignition cycle.

4. CONCLUSIONS

The feasibility of operating a compression ignition natural gas engine using partial replacement of nitrogen with argon as the working fluid was numerically evaluated, and the following represent the major outcomes of this study:

- In the current engine with the specified operating conditions, the auto-ignition of natural gas does not occur when air is the working fluid. However, partial replacement of nitrogen with argon results in auto-ignition and combustion. Although abnormal combustion and quite long ignition delays are observed for 10 and 20 percent replacement, a more practical engine cycle is achievable when more than 30 percent argon is added to the intake.
- Increasing the amount of argon in the intake gas composition leads to the reduction in ignition delay and heat release rate. Additionally, it increases the peak pressure, in-cylinder temperature, and combustion duration. The main reason for the abovementioned effects is the lower specific heat of argon compared to nitrogen, which enables the mixture to reach higher temperatures during compression.
- H_2O_2, HO_2, and OH radicals play an important role in ignition and onset of combustion. The investigation of species history indicates that the increase in temperature leads to the decomposition of H_2O_2, and production of OH radicals, which initiates the flame. This follows the fundamental chemical kinetics argument in intermediate temperature ignition applications.
- The composition of the products shows that argon, nitrogen, and oxygen are the main products of this cycle (more than 96%), and water vapor and carbon dioxide are the minor products which can be separated through condenser and membrane. The remaining argon, nitrogen, and oxygen can be recirculated to the inlet manifold for the next cycle. The excess amount of oxygen in the products is due to the extremely lean operating conditions of this engine (overall equivalence ratio of 0.09).

NOMENCLATURE

A	Pre-exponential factor
AMR	Adaptive mesh refinement
aTDC	After top dead center
b	Temperature exponent
BDC	Bottom dead center
CA	Crank angle
CFD	Computational fluid dynamics
CFL	Courant-Friedrichs-Lewy
DME	Dimethyl ether
E_a	Activation energy

EGR	Exhaust gas recirculation
EVO	Exhaust valve open
HC	Unburned hydrocarbons
HCCI	Homogeneous charge compression ignition
HRR	Heat release rate
IMEP	Indicated mean effective pressure
IVC	Intake valve close
k	Reaction coefficient
M	Third body
MP	Methyl propanoate
NG	Natural gas
NOx	Oxides of nitrogen
R_u	Universal gas constant
RANS	Reynolds-averaged Navier-Stokes
RCCI	Reactivity controlled compression ignition
RCM	Rapid compression machine
RME	Rapeseed methyl ester
RNG	Re-normalization group
SOI	Start of injection
TDC	Top dead center

ACKNOWLEDGEMENTS

This material is based upon work supported by Columbia Gas of Massachusetts under award #29797 with the University of Massachusetts Lowell. The authors would like to acknowledge Dr. Mohd Radzi Abu Mansor for his guidance on the numerical simulation. The authors would like to appreciate CONVERGE CFD software licensing team for their support.

REFERENCES

[1] S. Di Pascoli, A. Femia, and T. Luzzati, "Natural gas, cars and the environment. A (relatively)‘clean’and cheap fuel looking for users," *Ecological Economics,* vol. 38, no. 2, pp. 179-189, 2001.

[2] A. Sobiesiak and S. Zhang, "The first and second law analysis of spark ignition engine fuelled with compressed natural gas," SAE Technical Paper, 0148-7191, 2003.

[3] D. S. Ting and M. D. Checkel, "The effects of turbulence of spark-ignited, ultra lean, premixed methane-air flame growth in a combustion chamber," SAE Technical Paper, 0148-7191, 1995.

[4] L. H. Borges, C. Hollnagel, and W. Muraro, "Development of a Mercedes-Benz natural gas engine M 366 LAG, with a lean burn combustion system," SAE Technical Paper, 0148-7191, 1996.

[5] M. P. Hekkert, F. H. Hendriks, A. P. Faaij, and M. L. Neelis, "Natural gas as an alternative to crude oil in automotive fuel chains well-to-wheel analysis and transition strategy development," *Energy policy,* vol. 33, no. 5, pp. 579-594, 2005.

[6] M. Darzi, D. Johnson, C. Ulishney, and N. Clark, "Low pressure direct injection strategies effect on a small SI natural gas two-stroke engine’s energy distribution and emissions," *Applied energy,* vol. 230, pp. 1585-1602, 2018.

[7] S. Szwaja, E. Ansari, S. Rao, M. Szwaja, K. Grab-Rogalinski, J. D. Naber, M. Pyrc, "Influence of exhaust residuals on combustion phases, exhaust toxic emission and fuel consumption from a natural gas fueled spark-ignition engine," *Energy Conversion and Management,* vol. 165, pp. 440-446, 2018.

[8] M. Reyes, F. Tinaut, B. Giménez, and A. Pérez, "Characterization of cycle-to-cycle variations in a natural gas spark ignition engine," *Fuel,* vol. 140, pp. 752-761, 2015.

[9] H. M. Cho and B.-Q. He, "Spark ignition natural gas engines—A review," *Energy conversion and management,* vol. 48, no. 2, pp. 608-618, 2007.

[10] D. Flowers, S. Aceves, C. Westbrook, J. Smith, and R. Dibble, "Detailed chemical kinetic simulation of natural gas HCCI combustion: gas composition effects and investigation of control strategies," *Journal of engineering for gas turbines and power,* vol. 123, no. 2, pp. 433-439, 2001.

[11] Z. M. Hammond, J. H. Mack, and R. W. Dibble, "Effect of hydrogen peroxide addition to methane fueled homogeneous charge compression ignition engines through numerical simulations," *International Journal of Engine Research,* vol. 17, no. 2, pp. 209-220, 2016.

[12] A. Y. Nobakht, R. K. Saray, and A. Rahimi, "A parametric study on natural gas fueled HCCI combustion engine using a multi-zone combustion model," *Fuel,* vol. 90, no. 4, pp. 1508-1514, 2011.

[13] E. Pipitone and G. Genchi, "NOx reduction and efficiency improvements by means of the Double Fuel HCCI combustion of natural gas–gasoline mixtures," *Applied Thermal Engineering,* vol. 102, pp. 1001-1010, 2016.

[14] M. F. Ahari and E. Neshat, "Advanced analysis of various effects of water on natural gas HCCI combustion, emissions and chemical procedure using artificial inert species," *Energy,* vol. 171, pp. 842-852, 2019.

[15] E. Ansari, K. Poorghasemi, B. K. Irdmousa, M. Shahbakhti, and J. Naber, "Efficiency and Emissions Mapping of a Light Duty Diesel-Natural Gas Engine Operating in Conventional Diesel and RCCI Modes," SAE Technical Paper, 0148-7191, 2016.

[16] A. Paykani, A.-H. Kakaee, P. Rahnama, and R. D. Reitz, "Effects of diesel injection strategy on natural gas/diesel reactivity controlled compression ignition combustion," *Energy,* vol. 90, pp. 814-826, 2015.

[17] K. Poorghasemi, R. K. Saray, E. Ansari, B. K. Irdmousa, M. Shahbakhti, and J. D. Naber, "Effect of diesel injection strategies on natural gas/diesel RCCI combustion characteristics in a light duty diesel engine," *Applied Energy,* vol. 199, pp. 430-446, 2017.

[18] A.-H. Kakaee, P. Jafari, and A. Paykani, "Numerical Study of Natural Gas/Diesel Reactivity Controlled Compression Ignition Combustion with Large Eddy

Simulation and Reynolds-Averaged Navier–Stokes Model," *Fluids,* vol. 3, no. 2, p. 24, 2018.

[19] T. Korakianitis, A. Namasivayam, and R. Crookes, "Natural-gas fueled spark-ignition (SI) and compression-ignition (CI) engine performance and emissions," *Progress in energy and combustion science,* vol. 37, no. 1, pp. 89-112, 2011.

[20] A. Carlucci, A. d. de Risi, D. Laforgia, and F. Naccarato, "Experimental investigation and combustion analysis of a direct injection dual-fuel diesel–natural gas engine," *Energy,* vol. 33, no. 2, pp. 256-263, 2008.

[21] Z. Wang, Z. Zhao, D. Wang, M. Tan, Y. Han, Z. Liu, H. Dou, "Impact of pilot diesel ignition mode on combustion and emissions characteristics of a diesel/natural gas dual fuel heavy-duty engine," *Fuel,* vol. 167, pp. 248-256, 2016.

[22] R. Papagiannakis and D. Hountalas, "Combustion and exhaust emission characteristics of a dual fuel compression ignition engine operated with pilot diesel fuel and natural gas," *Energy conversion and management,* vol. 45, no. 18-19, pp. 2971-2987, 2004.

[23] M. Shahsavan, M. Morovatiyan, and J. H. Mack, "Numerical Study on Direct Injection of Hydrogen-Methane Blends into a Constant Volume Combustion Chamber," presented at the 11th US National Combustion Meeting, Pasadena, CA, 2019.

[24] T. Korakianitis, A. Namasivayam, and R. Crookes, "Diesel and rapeseed methyl ester (RME) pilot fuels for hydrogen and natural gas dual-fuel combustion in compression–ignition engines," *Fuel,* vol. 90, no. 7, pp. 2384-2395, 2011.

[25] Z. Chen, M. Konno, M. Oguma, and T. Yanai, "Experimental study of CI natural-gas/DME homogeneous charge engine," *SAE transactions,* pp. 442-451, 2000.

[26] S. Jouzdani, X. Zheng, D. M. Coombs, and B. Akih-Kumgeh, "Methane and Methyl Propanoate High-Temperature Kinetics," *Energy & Fuels,* vol. 32, no. 11, pp. 11864-11875, 2018.

[27] R. W. Dibble, M. S. Aznar, T. B. Sennott, and J.-Y. Chen, "Recirculating Noble Gas Internal Combustion Power Cycle," ed: Google Patents, 2017.

[28] M. Sierra-Aznar, D. I. Pineda, B. S. Cage, X. Shi, J. P. Corvello, J. Chen, R. W. Dibble, "Working fluid replacement in gaseous direct-injection internal combustion engines: A fundamental and applied experimental investigation," presented at the 10th US National Combustion Meeting, College Park, MD, 2017.

[29] M. Shahsavan, M. Morovatiyan, and J. H. Mack, "A numerical investigation of hydrogen injection into noble gas working fluids," *International Journal of Hydrogen Energy,* vol. 43, no. 29, pp. 13575-13582, 2018.

[30] M. Shahsavan, M. Morovatiyan, and J. H. Mack, "A Computational Investigation of Nonpremixed Combustion of Natural Gas Injected Into Mixture of Argon and Oxygen," *Journal of Engineering for Gas Turbines and Power,* vol. 141, no. 8, p. 081011, 2019.

[31] M. S. Aznar, F. Chorou, J.-Y. Chen, A. Dreizler, and R. W. Dibble, "Experimental and Numerical Investigation of the Argon Power Cycle," in *ASME 2018 Internal Combustion Engine Division Fall Technical Conference*, 2018: American Society of Mechanical Engineers, pp. V001T01A006-V001T01A006.

[32] N. M. Hafiz, M. R. A. Mansor, and W. M. F. Wan Mahmood, "Simulation of the combustion process for a CI hydrogen engine in an argon-oxygen atmosphere," *International Journal of Hydrogen Energy,* vol. 43, no. 24, pp. 11286-11297, 2018.

[33] S. Rey, "Study on the SI-CI Combustion and the Spontaneous Ignition of Hydrogen Jets using a Rapid Compression/Expansion Machine," Kyoto University, 2014.

[34] C. K. Westbrook, "Chemical kinetics of hydrocarbon ignition in practical combustion systems," *Proceedings of the combustion institute,* vol. 28, no. 2, pp. 1563-1577, 2000.

[35] S.-C. Kong, "A study of natural gas/DME combustion in HCCI engines using CFD with detailed chemical kinetics," *Fuel,* vol. 86, no. 10-11, pp. 1483-1489, 2007.